Morphology and Properties of *trans*-1,4-Polyisoprene Crystallized from Solution

Chen-Chih Kuo and Arthur E. Woodward*

Chemistry Department, The City University of New York, City College, New York, New York 10031. *Received May 2, 1983*

ABSTRACT: *trans*-1,4-Polyisoprene (TPI) fractions with $\bar{M}_n = 4.7 \times 10^3$ to 2.5×10^5 and $\bar{M}_w/\bar{M}_n = 2.0$–1.3 were crystallized from solutions, mainly at a concentration of 1 g/100 cm^3, by cooling directly from 100 °C to an (apparent) T_C of −15 to +32 °C, by precooling to 0 °C, redissolving at 35–45 °C, and crystallizing at T_C, and by cooling to 0 °C and heating to 10, 20, or 30 °C. Most of the structures obtained were characterized, while suspended in the crystallization liquid, by interference contrast microscopy and with crossed polaroids; the crystalline fraction from the density and the crystal form from X-ray diffraction and differential scanning calorimetry were determined for the dry products. The morphology obtained by direct crystallization was dependent on molecular weight, crystallization temperature, and solvent, with α- and β-hedrites (sheaves), α- and β-spherulites, and β-aggregates of cup-shaped lamellas being found. The precooling method yielded overgrown lamellas in most cases; however, more complex morphologies developed when the thermal history was changed. The density depended on molecular weight, concentration, and crystallization temperature. The crystallinity was mainly a function of crystal form and molecular weight. The equation of Tseng, Herman, Woodward, and Newman was used to explain the molecular weight dependence of the crystallinity at low $\bar{M}_n$ and to calculate the average number of monomer units per fold and interlamellar traverse. Epoxidation of some TPI structures suspended in amyl acetate at 0 °C was carried out. At high concentrations of the epoxidizing agent, *m*-chloroperbenzoic acid, the fraction epoxidized approached or exceeded the noncrystalline fraction as obtained from density measurement.

Introduction

The crystallization of *trans*-1,4-polyisoprene from solution has received some attention to date.[1-5] The morphology described in the greatest detail is that of single lamellas obtained from dilute solution,[2-5] although some complex structures have been observed.[1] Two crystalline forms, monoclinic (α) and orthorhombic (β), have been reported for this polymer,[6-8] and lamellas of both have been characterized.[2,5] Transformation from the β- to the α-form in the presence of a liquid has been reported.[4,9] The effect of molecular weight and crystallization temperature on the DSC melting endotherm for lamellas obtained by a precooling (or self-seeding) method for dilute solution and for structures prepared by direct cooling from an elevated temperature has been studied; the densities of the dilute-solution-grown lamellas have also been investigated.[5]

The morphology of polymers crystallized directly, without self-seeding, usually from moderately concentrated solutions, is found to be of a complexity between that of single lamellas and the multilamellar bodies obtained from the melt.[10,11] When suspended in the crystallization liquid, these structures can usually be observed and characterized individually by optical microscopy. However, the effects of molecular weight and crystallization temperature on the morphology and the systematic measurements of physical properties of these multilamellar structures from solution have received little attention to date. The 1,4-diene polymers are of particular interest because of the chemical reactivity due to the double bonds present. This has been previously used to investigate the morphology of melt-crystallized structures[12,13] as well as to assay the fraction of monomer units present at the surfaces of solution-grown lamellas.[5,14-17]

In the work to be presented herein, gutta percha fractions with number-average molecular weights of 4.7×10^3 to 2.5×10^5 were crystallized mainly from amyl acetate solution using a concentration of 1 g/100 cm^3 at temperatures in the −15 to +32 °C range. The morphology of the structures prepared was investigated by interference contrast optics and with crossed polaroids in the presence of the crystallization liquid or by electron microscopy. For most of these preparations the crystallinity from the density and the crystal form, as obtained from X-ray photographs and differential scanning calorimetry endotherms, were determined. Finally, some preparations were subjected to an epoxidation reaction in suspension to determine the surface fraction of the polymer structure available for reaction, with the extent of reaction being determined by ^{1}H NMR.

Experimental Section

Samples. Gutta percha was obtained from Gabungan Produsen Karet, Indonesia. Following extraction with acetone, fractionation was carried out either by methanol precipitation from toluene solution[4,5] or by extraction of the polymer on a diatomaceous earth column using amyl acetate–2-ethoxyethanol mixtures,[5] both in the presence of 2,2′-methylenebis[4-methyl-6-*tert*-butylphenol)] as antioxidant. The molecular weights and polydispersities of the fractions used in this work, as measured by gel permeation chromatography,[4] are as follows ($\bar{M}_n \times 10^{-5}$, $\bar{M}_w/\bar{M}_n$): 2.5, 1.3; 1.3, 1.5; 1.2, 1.2; 1.0, 1.6; 0.24, 1.5; 0.23, 1.3; 0.099, 2.0; 0.049, 1.3; 0.047, 1.3.

Crystallization. Two crystallization procedures were employed and are referred to below as the direct and the precooling methods, respectively. In the direct crystallization method the sample was heated in the crystallization liquid to 100 °C, filtered, held at that temperature for 1 h, and then cooled in a constant-temperature bath to the crystallization temperature, T_C. In the precooling method the heated solution was cooled in ice water or a dry ice–acetone mixture, bringing about precipitation; after cooling to 0 °C the polymer–liquid mixture was heated at a rate of approximately 0.2 °C min^{-1} to the minimum redissolution temperature, T_R, followed by a second cooling to T_C. T_R is found to increase with molecular weight; for a 1% (w/v) solution in amyl acetate it is 35 °C for $\bar{M}_n = 4700$ and 45 °C for $\bar{M}_n = 2.5 \times 10^5$. In some other experiments the precipitated polymer–liquid mixture at 0 °C was heated at various rates to a temperature below the redissolution temperature. Following a 1-day crystallization or recrystallization period, the polymer was recovered by filtration, with washing and drying under vacuum carried out at the final crystallization temperature. In most of the crystallizations a concentration of 1 g in 100 cm^3 ($W_2 = 0.011$) was used and amyl acetate was the crystallization liquid employed; concentrations of 0.05, 3.0, and 8.0 were also used. In a few cases heptane or dibutyl ether was used as the crystallization liquid.

Morphology. Most of the crystal preparations were studied both by interference contrast optical microscopy and with crossed polaroids prior to drying. Electron microscopy was carried out

0024-9297/84/2217-1034$01.50/0

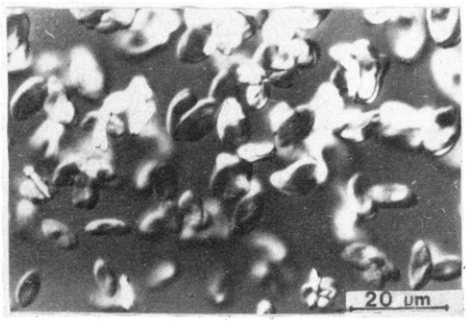

Figure 1. Interference contrast photomicrograph for α-TPI hedrites from amyl acetate in suspension (1 g/100 cm^3 concentration, $\bar{M}_n = 2.4 \times 10^4$, $T_C = 20$ °C).

on some samples shadowed with Pt/Pd after drying on carbon-coated grids and on one sample treated with OsO_4 in amyl acetate solution prior to drying.

Crystal Form. Wide-angle X-ray diffraction using a 57.3-mm-diameter camera and differential scanning calorimetry with a DuPont 990 thermal analyzer were employed to identify the crystal form(s) present.

Crystallinity. The crystalline fraction was obtained from the sample density using literature values of the amorphous[18] and crystalline densities[6-8] ($\rho_A = 0.905$ g cm^{-3}, $\rho_C(\alpha) = 1.05$ g cm^{-3}, and $\rho_C(\beta) = 1.02$ g cm^{-3}). The density was measured at 25 °C with an ethanol–water density gradient apparatus. All samples were pressed at 3.4×10^7 Pa to eliminate air.

Surface Fraction. Reaction of the available double bonds with *m*-chloroperbenzoic acid (MCPBA) in amyl acetate suspension at 0 °C was used to assess the surface fraction. The reaction was carried out with enough MCPBA present to react with 80% of the double bonds present before crystallization. Starting concentrations of 0.2–2.0 g of MCPBA per 100 cm^3 of amyl acetate and reaction times of 0.5–28 days were used. The epoxidized polymer after washing with amyl acetate and then with ether was dried at 0 °C and subsequently subjected to ^{1}H NMR measurement in $CDCl_3$ solution at room temperature using a JEOL JNM MH100. The fraction epoxidized was obtained from the area under the resonances at 2.7 ppm for the epoxidized CH and at 5.1 ppm for unepoxidized CH.

Results

Morphological Studies. *trans*-1,4-Polyisoprene fractions with molecular weights $\bar{M}_n = 2.4 \times 10^4$, 1.0×10^5, and 2.5×10^5 were used for the morphological examinations. A majority of the preparations examined were grown from amyl acetate solution by direct crystallization at T_C values between −15 and +32 °C at a concentration of 1.0 g/100 cm^3. Morphological examination was carried out in the presence of crystallization liquid by both interference contrast and crossed-polaroid optical microscopy. The morphology observed was found to depend on the crystallization method and the final T_C, the choice of crystallization liquid, and the molecular weight. The structures obtained are classified in terms of the appearance under interference contrase optics and the crystal form as found from X-ray diffraction and DSC endotherm temperatures. For the lowest molecular weight used ($\bar{M}_n = 2.4 \times 10^4$) two types of structures appeared. At T_C's of 15, 20–21, and 32 °C structures in the α-form, as shown in Figure 1, were observed. These are relatively small multilamellar bodies of elliptical shape with little, if any, birefringence face on but with strong birefringence from the side. These are classified herein as hedrites.[10] Due to the high solubility of this fraction at 32 °C a concentration of 3.0 g/100 cm^3 of solvent was used. At T_C's of −15, 0, +10, and +15 °C larger more complex structures were generally observed, an example being given in Figure 2; the same field was observed by interference contrast and crossed polaroids. These photographs contain one structure viewed face-on

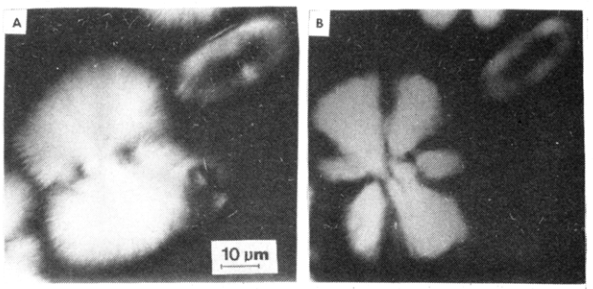

Figure 2. Interference contrast (a) and cross-polaroid (b) photomicrographs of β-TPI hedrites from amyl acetate in suspension (1 g/100 cm^3 concentration, $\bar{M}_n = 2.4 \times 10^4$, $T_C = 10$ °C).

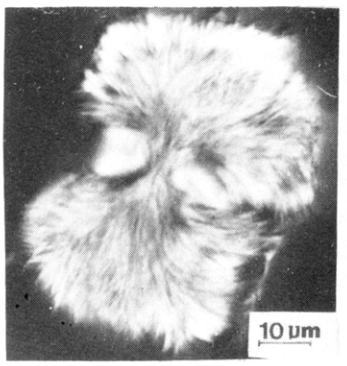

Figure 3. Same as Figure 1 except $\bar{M}_n = 2.5 \times 10^5$ and $T_C = 20$ °C.

(oval shape) and the other from the side of the sheaf; observation of these as they rotate in the crystallization liquid confirmed that they are different views of similar bodies. Rotation of the microscope stage during observation under crossed polaroids produced changes in the birefringence pattern.

The β-form was found to be the only form present for the lowest molecular weight at T_C's of −15 and 0 °C; β is the predominant form at a T_C of 10 °C and present in about equal amount with the α-form at 15 °C. As reported earlier[4] the structures grown from this molecular weight at a T_C of 0 °C show two endotherms at 42 and 53 °C when the product is collected after the usual time period of 1 day. If the crystals are collected 15 min after crystallization commences, only the endotherm at 53 °C is found and the β-form is the only form present. It was observed that precipitation commences before the solution reaches 0 °C, indicating that nonisothermal conditions prevailed during the early stages.

The morphological results on the highest molecular weight fraction studied, $\bar{M}_n = 2.5 \times 10^5$, differed from the above. A photomicrograph of a structure crystallized at 20 °C at a concentration of 1 g/100 cm^3 is shown in Figure 3. The morphology of structures obtained at 32 °C was similar, although they were smaller in size. DSC and X-ray diffraction indicated the presence of the α-form at these two crystallization temperatures. At a T_C of 10 °C twisted and branched but spherically symmetrical structures in the β-form showing strong scattered birefringence were prepared. (See Figure 4 for representative morphology and birefringence.)

For a molecular weight of 2.5×10^5 when T_C is 0 or −15 °C the morphological structures are aggregates of cup-shaped lamellas as shown in Figures 5 and 6. At 1 g/100 cm^3 these aggregates are densely packed but at a lower concentration (0.05 g/100 cm^3) individual cup-shaped structures in each aggregate can be identified. At −15 °C some single cup-shaped lamellas also exist. Crystallization was observed to start before the solution reaches 0 °C,

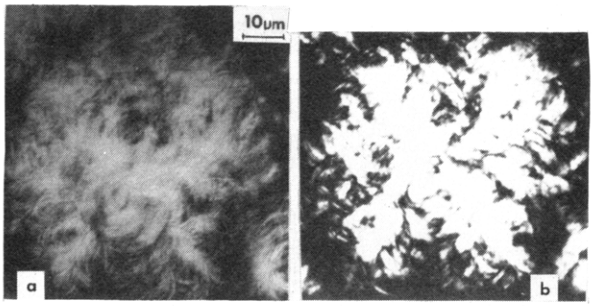

Figure 4. Interference contrast (a), and crossed-polaroid (b) photomicrographs for β-TPI spherulites from amyl acetate in suspension (1 g/100 cm^3 concentration, $\bar{M}_n = 2.5 \times 10^5$, $T_C = 10$ °C).

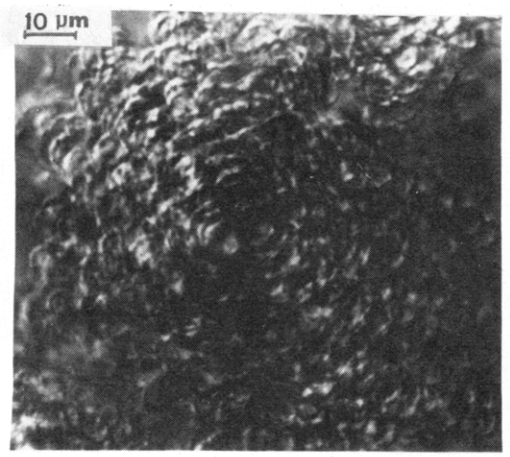

Figure 5. Interference contrast photomicrograph for β-TPI aggregate from amyl acetate in suspension (1 g/100 cm^3 concentration, $\bar{M}_n = 2.5 \times 10^5$, $T_C = 0$ °C).

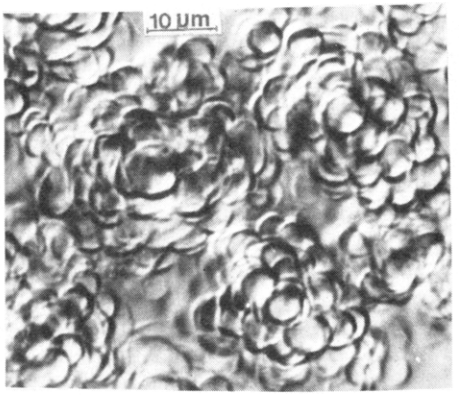

Figure 6. Same as Figure 5 but 0.05 g/100 cm^3 concentration.

indicating that nonisothermal conditions prevail. At the onset of crystallization cup-shaped lamellas appear in the optical microscope followed by growth of other such lamellas about the initial one. In order to investigate these aggregates at higher magnifications in the absence of the crystallization liquid, the suspension obtained at 0.05 g/100 cm^3 was mixed with osmium tetraoxide in amyl acetate, and the mixture was washed and dried; optical and electron microscopy was then carried out. Typical electron micrographs are shown in Figure 7 for the 0.05 g/100 cm^3 preparation. The lamellar nature of these cup-shaped structures is evident therein. Due to the larger number of overgrowths the individual structures in the 1 g/100 cm^3 preparation are thicker and show less detail under the electron microscope. Some evidence of lamellar strips connecting the cup-shaped lamellas was found in the optical micrographs. X-ray diffraction and DSC scans, the

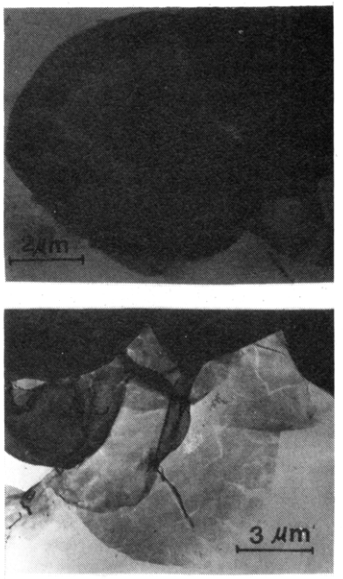

Figure 7. Electron micrographs of OsO_4-treated β-TPI aggregates from amyl acetate (0.05 g/100 cm^3 concentration, $\bar{M}_n = 2.5 \times 10^5$, $T_C = 0$ °C).

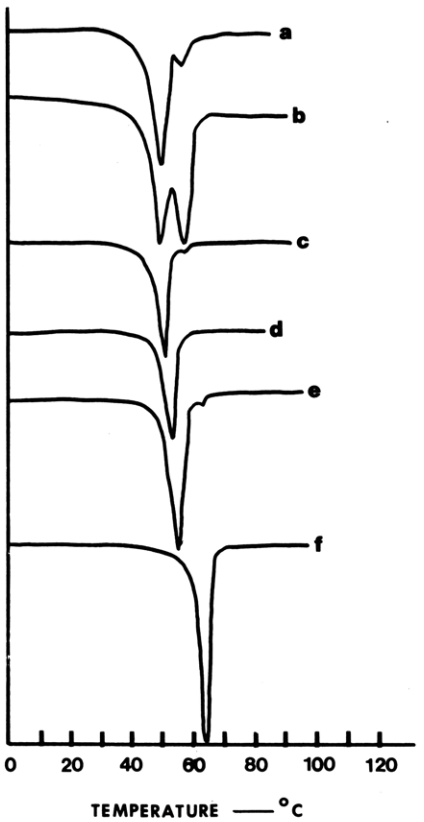

Figure 8. DSC scans for dry TPI aggregates from amyl acetate ($\bar{M}_n = 2.5 \times 10^5$, $T_C = 0$ °C): (a) 0.05 g/100 cm^3 concentration; (b) 1.0 g/100 cm^3; (c) same but heated in suspension at 0.3 °C min^{-1} to 10 °C; (d) same but final temperature 20 °C; (e) same but final temperature 30 °C; (f) same but heating rate fast.

latter as given in Figure 8, indicate the presence of both α ($T_{endo} = 59$ °C) and β ($T_{endo} = 50$ °C) forms, with β predominating at the lower concentration used (0.05 g/100 cm^3). If, following precipitation at 0 °C at a concentration of 1 g/100 cm^3, the mixture is heated at a rate of 0.3 °C min^{-1} to 10, 20, or 30 °C, only a trace of the α-form is observed after drying, as seen from the DSC endotherms in Figure 8; however, the morphology remains substantially the same. This suggests that the α-form that appears in

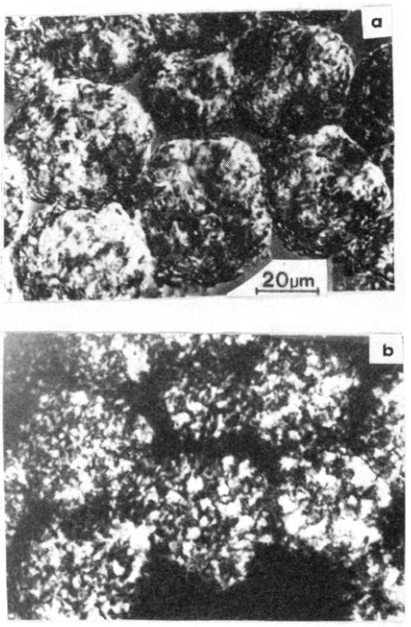

Figure 9. Interference contrast (a) and crossed-polaroid (b) photomicrographs of α-TPI spherulites from dibutyl ether in suspension (1 g/100 cm³ concentration, $\bar{M}_n = 2.5 \times 10^5$, $T_C = 0$ °C).

the $T_C = 0$ °C product is caused by crystallization or recrystallization upon drying at 0 °C. Rapid heating at 30 °C of the $T_C = 0$ °C preparation in the presence of the crystallization liquid leads to dissolution and precipitation of single lamellas in the α-form. When slow heating of this preparation to 35 °C was carried out, parts of the structures underwent dissolution followed by subsequent single-lamella precipitation while other parts remained but appeared damaged, at least near the surfaces, when viewed under the optical microscope; however, the crystal form for the dried sample was α.

Some morphological studies were made on structures from a fraction with $\bar{M}_n = 1.2 \times 10^5$, $\bar{M}_w/\bar{M}_n = 1.2$, crystallized at 0, 10, and 20 °C and from a fraction with $\bar{M}_n = 2.3 \times 10^4$, $\bar{M}_w/\bar{M}_n = 1.3$, crystallized at 20 °C. The morphologies occurring were similar to those found for samples with larger $\bar{M}_w/\bar{M}_n$ values (1.5 and 1.6).

Use of the precooling method with material having $\bar{M}_n = 2.5 \times 10^5$ with $T_D = 100$ °C, $T_P = 0$ °C, $T_R = 45$ °C, and $T_C = 0$–30 °C always led to the α-form[4] at a concentration of 1.0 g/100 cm³. However, the morphology obtained depends on the heating rate from T_P to T_R. A rate of 0.3 °C min⁻¹ with T_C of 0 or 20 °C yielded single lamellas, a rate of 0.5–0.6 °C min⁻¹ gave structures at $T_C = 20$ °C similar to those in Figure 1, and a rate faster than 0.6 °C min⁻¹ yielded structures at a T_C of 20 °C similar to that shown in Figure 3.

A few experiments were carried out with crystallization liquids other than amyl acetate. Direct crystallization from heptane or from dibutyl ether with $\bar{M}_n = 2.5 \times 10^5$ and a concentration of 1 g/100 cm³ at $T_C = 0$ °C yielded spherically symmetrical structures in the α-form as shown in Figure 9; these structures exhibit strong scattered birefringence. When material with $\bar{M}_n = 2.4 \times 10^4$ was employed with heptane as solvent, structures in the β-form similar to those in Figure 2 were formed.

The morphologies described above, in addition to single lamellas, have been classified as follows: I, sheaves in the α-form from amyl acetate (hedrites); IIa, sheaves in the β-form from amyl acetate and heptane (hedrites); IIb, spherulites in the β-form from amyl acetate; III, aggregates of cup-shaped lamellas in the β-form from amyl acetate; IV, spherulites in the α-form from heptane and dibutyl ether. The appearance of these morphologies at the molecular weights and crystallization temperatures used is summarized in Table I for direct amyl acetate crystallization.

Table I
Classification of Morphology of *trans*-1,4-Polyisoprene from Amyl Acetate Solution as a Function of Molecular Weight and Crystallization Temperature

	$\bar{M}_n$		
T_C, °C	2.4×10^4	1.0×10^5	2.5×10^5
32	I (α-hedrites (sheaves))		I
20–21	I	I	I
15	IIa (β-hedrites (sheaves)) and I	I and IIa	I
10	I and IIa	IIa	IIb (β-spherulites)
5	IIa	IIb	IIb
0	IIa	IIb	III (β-aggregates of cup-shaped lamellas)
−15	IIa	III	III

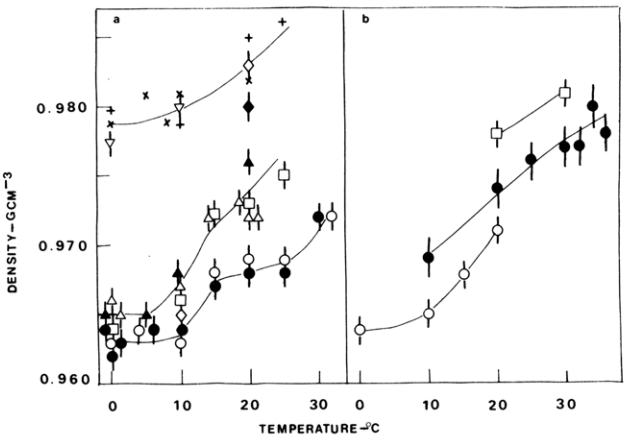

Figure 10. Density at 25 °C vs. crystallization temperature, T_C, for TPI. (a) Concentration 1 g/100 cm³ of amyl acetate: direct crystallization, (○) $\bar{M}_n = 2.5 \times 10^5$, (□) $\bar{M}_n = 1.0 \times 10^5$, (△) $\bar{M}_n = 2.4 \times 10^4$, (◇) $\bar{M}_n = 9.9 \times 10^3$, (▽) $\bar{M}_n = 4.9 \times 10^3$, (×) $\bar{M}_n = 4.7 \times 10^3$; precooled crystallization, (●) $\bar{M}_n = 2.5 \times 10^5$, (▲) $\bar{M}_n = 2.4 \times 10^4$, (◆) $\bar{M}_n = 9.9 \times 10^3$, (+) $\bar{M}_n = 4.7 \times 10^3$. (b) Concentration 0.05 g/100 cm³ of amyl acetate: direct crystallization, (○) $\bar{M}_n = 2.5 \times 10^5$; precooled crystallization, (●) $\bar{M}_n = 0.69 \times 10^5$ to 2.9×10^5 (ref 5), (□) $\bar{M}_n = 2.4 \times 10^4$ (ref 5).

Density Measurement and Sample Crystallinity. Density measurements for seven directly crystallized and twelve precooled preparations at various crystallization temperatures, T_C, are summarized in Figure 10. The density increases with increasing T_C and decreases with an increase in concentration from 0.05% to 1.0% (w/v) and with an increase in molecular weight. As noted in Table I in the 10–20 °C region for directly crystallized samples, a mixture of two different crystal structures with different densities can result. Density measurements were also made on (dried) cup-shaped lamellar crystal aggregates directly crystallized from 1% (w/v) amyl acetate solution at 0 °C using TPI with $\bar{M}_n = 2.5 \times 10^5$ and subsequently annealed in the crystallization liquid at 10, 20, and 30 °C. Two values for the rate of heating to the annealing temperature of 30 °C were used, 0.3 °C min⁻¹ (slow) and immediate immersion at 30 °C (fast), the former giving the β-form and latter the α-form. The densities obtained were 0.966, 0.968, and 0.972 g cm⁻³ for a heating rate of 0.3 °C min⁻¹ to 10, 20, and 30 °C while a value of 0.975 g cm⁻³ upon fast heating to 30 °C was measured. The melting endotherm value also increases with increasing

annealing temperature (see Figure 8).

Crystallinities (weight fraction) calculated from the density values obtained in this study are given in Table II for the preparations that yielded for the crystalline portion either the α- or the β-form. At the top of the table the crystal form(s) prepared are indicated. At the lower temperatures (0 and 10 °C) direct crystallization yields β and the precooling technique gives α. It is to be noted that at any temperature used the samples in the β-form show a significantly larger crystallinity than those in the α-form.

Epoxidation. The epoxidation of a portion of the double bonds in TPI structures crystallized from 1% (w/v) amyl acetate solution at 20–21 °C was carried out to various times for polymer with number-average molecular weights from 1.0×10^5 to 2.5×10^5 at various *m*-chloroperbenzoic acid concentrations ($[MCPBA]_{t=0}$). The mole ratio of MCPBA to double bonds was chosen so that a considerable excess of MCPBA was always present. The fraction of epoxidation taking place, as obtained by ^1H NMR, is given for each sample in Table III. Most of the epoxidations were carried out on type I structures (see above), although in three cases they were single lamellas prepared by the precooling method. After an initial stage, over in less than 6 days, little reaction takes place. However, there is an effect of $[MCPBA]_{t=0}$ on the total epoxidation fraction occurring; this fraction exceeds the noncrystalling fraction from density at high $[MCPBA]_{t=0}$ for both of the precooled and two of the three directly crystallized samples. A similar result was observed for dilute-solution-grown TPI lamellas prepared by the precooling method at a T_C of 20 °C.[5]

Discussion

It was demonstrated above that the morphology of *trans*-1,4-polyisoprene structures grown directly from solution depends on the crystallization temperature, T_C, the polymer molecular weight, and the solvent. Three structural types were observed: hedrites (sheaves) (at all T_C's dependent on $\bar{M}_n$), spherulites (at medium and low T_C and medium $\bar{M}_n$), and aggregates of curved lamellas (at low T_C and medium $\bar{M}_n$). Under isothermal crystallization conditions the hedrites formed become larger and more complex as the crystallization temperature decreases and/or the molecular weight increases for a particular solvent system and are apparently the precursors of spherulites. As the temperature is decreased, the polymer solubility decreases and the crystallization rate increases.[19] The faster growth leads to branching and twisting and therefore to more open, larger structures. Concerning the differences in birefringence observed in this work, an extinction cross (or double cross) was exhibited by some of the larger hedrite structures with an apparently larger polymer segment density; the structures giving these patterns are not spherically symmetrical. When T_C is 0 °C or lower, nonisothermal crystallization occurs for all molecular weights studied, leading to multiple endotherms.

Relatively thick elliptical and elongated hexagonal-shaped structures prepared in the α-form by a vapor diffusion method and by precipitation from solution were reported earlier by Schlesinger and Leeper.[1] Oval objects were prepared by Davies and Long[13] from the melt in the β-form using unfractionated TPI; the birefringence of these structures changes from no extinction to complete extinction upon rotation of the crystals. Changes in extinction on rotation without complete extinction were observed in this work. The oval structures obtained in the present work splay out, at least when in contact with the crystallizing liquid, and the thinner center portion shows extinction when viewed face-on at all orientations.

Table II
Weight Fraction Crystallinity of TPI Structures from Solution[a]

$\bar{M}_n$	crystal method	T_C, °C: 32	30	0/30 slow[b]	0/30 fast[b]	25	20	0/20 slow	10	0/10 slow	5	0
2.5×10^5	direct	0.52 (α)		0.63 (β)	0.54 (α)	0.50 (α)	0.49 (α)	0.60 (β)	0.56 (β)	0.58 (β)	0.56 (β)	
	precooled		0.52 (α)			0.49 (α)	0.49 (α)		0.45 (α)		0.46 (α)	0.46 (α)
1.0×10^5	direct					0.54 (α)	0.52 (α)		0.54 (β)			0.56 (β)
2.4×10^4	direct	0.52[c] (α)					0.52 (α)					0.58 (β)
	precooled						0.55 (α)		0.49 (α)		0.47 (α)	0.47 (α)
0.99×10^4	direct		0.57[d] (α)				0.60 (α)					
	precooled						0.57 (α)					
0.49×10^4	direct								0.70 (β)			0.68 (β)
0.47×10^4	direct						0.59[c] (α)		0.69 (β)			0.69 (β)
	precooled					0.62 (α)	0.61 (α)		0.57 (α)			0.57 (α)

[a] 1% w/v amyl acetate except where noted. [b] Slow and fast refer to heating rate from 0 to 30 °C (see text). [c] 3% w/v. [d] 8% w/v.

Table III
Epoxidation of TPI Crystallized from 1% (w/v) Amyl Acetate at T_C = 20–21 °C

$\bar{M}_n$	type[a]	crystallization method	$[MCPBA]_{t=0}$, % w/v	fraction epoxidized 6 days	10 days	12 days	16 days	21 days	22 days	28 days	F_S[b]
2.5×10^5	H	direct	0.10							0.45	0.50
	H	direct	1.0					0.56	0.55		
	S	precooled	1.0						0.58		
1.3×10^5	H	direct	0.20	0.28	0.29	0.28					
			2.0	0.64	0.59	0.57					
1.0×10^5	H	direct	0.20		0.22		0.22				0.48
			0.61		0.31						
			1.0		0.42			0.47			
			1.6		0.42			0.46			
			2.0		0.41			0.51			
	S	precooled	0.20		0.35						
			1.0		0.54						

[a] H, hedrites; S, single lamellas. [b] Noncrystalline fraction from density.

The cup-shaped lamellar aggregate morphology, grown under nonisothermal conditions at low T_C and medium molecular weights, differs markedly from the sheaflike (hedrite) structures, found at the same temperatures for a lower molecular weight sample. The retention of the cup-shaped morphology and of the β-structure that usually takes place upon slow heating in the crystallization liquid is caused by recrystallization to form thicker, more thermodynamically stable crystals with a higher melting point. If the annealing temperature is high enough, a solid-state β-to-α transition occurs in parts of the structures while in other parts melting of the β-form and precipitation of the α-form take place. Fast heating, on the other hand, leads only to melting, with the α-form subsequently crystallizing out. The formation of single and of aggregate cup-shaped lamellas has been cited previously for unfractionated poly(4-methyl-1-pentene)[20,21] (P4MP1), poly(oxymethylene),[22] and poly(chlorotrifluoroethylene)[23] crystallized at relatively large supercoolings. For unfractionated P4MP1 with $\bar{M}_n = 2.5 \times 10^5$ the morphology was found to change from square to curved as the supercooling increased. The model put forth to explain the increase in curvature of poly(4-methyl-1-pentene) crystals with increased supercooling contained the combined influence of two factors; these are a fold domain buckling due to chain-fold bulkiness and the lateral size of fold domains in the multisectored lamellas formed.[21] In the present work using *trans*-1,4-polyisoprene the change is from (ribbonlike) multilamellar structures to connected cup-shaped lamellas; this is molecular weight dependent.

Although the α-crystal form usually results, the morphology appearing for precooled solutions was reported herein to depend on the heating rate from the initial precipitation temperature (0 °C) to the redissolution temperature (45 °C); the appearance of more complex structures, when the heating rate is fast, is due possibly to a loss of a larger number of crystal nuclei during the heating process.

The morphology of melt-crystallized polyethylene and poly(ethylene oxide)[24,25] was found to be strongly dependent on polydispersity and molecular weight. Therefore morphologies other than those reported herein for *trans*-1,4-polyisoprene from solution or the melt may well be possible, since the molecular weights used in this study were limited to only 1 decade and the $\bar{M}_w/\bar{M}_n$ values were 1.2 or greater.

It was found in this study that hedrites, spherulites, and cup-shaped lamellar aggregates in the β-form have a significantly higher crystallinity than hedrites or overgrown lamellas in the α-form when the same final (crystallization or annealing) temperature is used. This difference is found to be about 20% and suggests that the lamellar thickness for crystals in the β-form is larger than that for those in the α-form. The measured thickness for β-lamellas grown from the melt using nonfractionated TPI were reported by Davies and Long[26] as larger than those for α-form lamellas grown at the same T_C; at a T_C of 50 °C $(L_\beta - L_\alpha)/L_\beta$ for melt-crystallized TPI is about 20%, in agreement with the crystallinity difference cited above for solution-grown crystals.

An increase in crystallinity of about 20–30% is found with decreasing molecular weight below about 10^4 for both the α- and β-forms. An increase in crystallinity with decreasing molecular weight down to about $\bar{M}_n = 10^4$ was reported for polyethylene[27,28] and for various poly(alkylene oxides)[29–32] crystallized from the melt. However, at molecular weights below 10^4 a decrease in crystallinity occurs for a number of these polymers, including polyethylene,[28] poly(ethylene oxide),[30] and poly(hexamethylene oxide).[31] Also a decrease in crystallinity with decreasing molecular weight in the 5000–30 000 range was reported for *trans*-1,4-polybutadiene.[16,17]

The noncrystalline component is expected to consist of chain folds, chain ends, interlamellar links, and intralamellar defects. Assuming intralamellar defects to be negligibly small, the noncrystalline fraction is given by[16]

$$F_S = \{UF + C\}/\bar{N}_n \quad (1)$$

where U is the average number of monomer units per fold and interlamellar traverse combined, F is the number of folds and interlamellar traverses per chain with a number-average degree of polymerization of $\bar{N}_n$, and C is the average number of monomer units in the two chain ends. The crystalline fraction, $1 - F_S$, is related to the above parameters and to the crystalline stem length, L_C, by

$$1 - F_S = (L_C/R\bar{N}_n)(F + 1) \quad (2)$$

where R is the crystallographic repeat distance in the chain direction. Equations 1 and 2 can be combined to eliminate F, giving

$$1 - F_S = (L_C/R)\{1 + (U - C)/\bar{N}_n\}/\{U + L_C/R\} \quad (3)$$

At large $\bar{N}_n$, $(U - C)/\bar{N}_n$ will be much smaller than 1 and the crystalline fraction $1 - F_S$, will be independent of $\bar{N}_n$ and will be constant with changing $\bar{N}_n$ if L_C and U remain constant. At low $\bar{N}_n$, $1 - F_S$ will change with a change in $\bar{N}_n$ and the direction of this will depend on the relative values of C and U. If C is greater than U, then $1 - F_S$ decreases as $\bar{N}_n$ decreases (at constant U and L_C/R), as was found for *trans*-1,4-polybutadiene lamellas.[16] The observed increase in crystallinity with decreasing molecular

Table IV
Average Number of Monomer Units per Fold and Interlamellar Traverse, U, for α-TPI from 1% Amyl Acetate Solution

T_C, °C	$\bar{M}_n$	L,[a] nm	L_C,[b] nm	U
10	2.5×10^5	7.8	3.2	8.9
20	1.0×10^5	9.0	4.3	9.0
	2.5×10^5	9.0	4.1	9.7
25	1.0×10^5	11.5	5.8	11
	2.5×10^5	11.5	5.2	12
30	2.5×10^5	12.5	6.0	13

[a] Lamellar thickness from electron microscopy.[5] [b] Crystal thickness from L using eq 5.

weight for α-TPI at T_C's of 10–30 °C suggests that the average length of the noncrystallizing chain ends, $C/2$, is small with respect to $U/2$. As discussed below, the U values for α-TPI structures prepared in this work range from 9 to 13. Therefore the maximum molecular weight at which a change in crystallinity should occur with changing $\bar{M}_n$, with the crystallinity expressed to two significant figures, is about 9×10^4. However, the results in Table II show a decrease in crystallinity as $\bar{M}_n$ increases up to 2.5×10^5 at T_C's of 20 and 25 °C, suggesting that a change in U and also L_C/R is taking place at larger molecular weights. It was reported earlier[5] that α-TPI lamellas grown from dilute amyl acetate solution using the precooling method show no consistent change in crystallinity with molecular weight in the 3.8×10^5 to 6.9×10^4 range.

In order to analyze the crystallinity results in a more quantitative manner, U values are calculated for the α-form structures with $\bar{M}_n$'s of 1.0×10^5 and above using the following expression, obtained from eq 3 when $\bar{N}_n$ is large:[16]

$$U = L_C/R\{F_S/(1 - F_S)\} \quad (4)$$

The $1 - F_S$ values are taken as equal to the crystalline fraction as obtained from density, and R is 0.439 nm.[8] A value for the parameter L_C is also needed for this calculation; this is obtained from the lamellar thickness, L, measured by electron microscopy for dilute-solution-grown TPI lamellas,[5] using the relationship[16]

$$L_C = (1 - F_S)\rho_A L/\{(1 - F_S)\rho_A + F_S\rho_C\} \quad (5)$$

Values of U and L_C obtained for α-TPI at T_C's of 10–30 °C are given in Table IV. The U values are found to increase with increasing T_C, as reported earlier for dilute-solution-grown α-TPI lamellas.[5] An increase in U with increasing molecular weight, as suggested above, is also observed. To demonstrate that the variation of the crystallinity with molecular weight below $\bar{M}_n = 10^5$ is principally due to replacement of chain folds by short chain ends, eq 3 was used to calculate the crystallinity assuming U and L_C/R are constant and C is zero. The U and L_C values used were those found at $\bar{M}_n = 1 \times 10^5$ for samples prepared at crystallization temperatures of 20 and 25 °C (see Table IV). For $T_C = 10$ °C it was necessary to calculate U and L_C/R at $\bar{M}_n = 2.4 \times 10^4$ for $T_C = 10$ °C due to the lack of a density value at $\bar{M}_n = 1 \times 10^5$. In Figure 11 the $1 - F_S$ values calculated from eq 3, represented by solid lines, are compared with those calculated from the density. Density-derived values for α-TPI crystallized from dilute solution by the precooling method[5] are also included. Except for the structures obtained with material with $\bar{M}_n = 2.5 \times 10^5$ at a 1% (w/v) concentration at all crystallization temperatures, the density-derived crystallinities are well represented by eq 3. Choice of a C value greater than zero would yield lower calculated values for $1 - F_S$ of structures with $\bar{M}_n$ below 10^5.

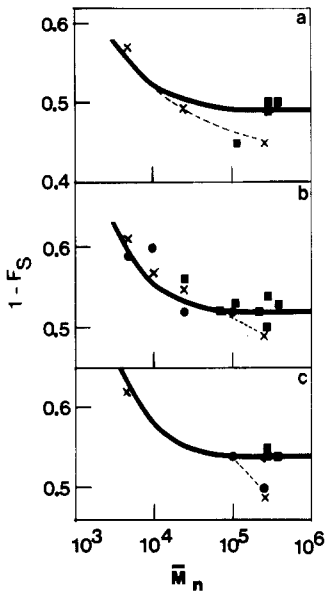

Figure 11. Crystalline fraction vs. log $\bar{M}_n$ for α-TPI structures from amyl acetate at T_C = 10, 20, and 25 °C (a, b, and c, respectively): (×) crystallized by precooling method from 1% (w/v) solution; (●) crystallized directly from 1% (w/v) solution; (■) crystallized by precooling method from 0.05% (w/v) solution;[5] (—) calculated with eq 3.

The crystallinity shows little, if any, change with a change in TPI morphology from hedrites (direct crystallization) to single but overgrown lamellas (precooled preparations) at constant molecular weight and crystallization temperature. This suggests that any interlamellar links present in the multilamellar structures contain about the same average number of monomer units as found in a fold.

The near constancy of the crystalline fraction for structures in either the α- or β-forms at 0 °C for $\bar{M}_n$'s between 2.5×10^5 and 2.4×10^4 is apparently a consequence of the nonisothermal crystallization conditions.

In order to explain the molecular weight dependence of the crystallinity for melt-crystallized polyethylene, poly(ethylene oxide), and poly(hexamethylene oxide) using eq 3, a decrease in U with decreasing $\bar{N}_n$ at large $\bar{N}_n$ values must be postulated. This does not necessarily mean that the average number of monomer units per fold is decreasing, since U is composed of two parts and changes may be occurring in the number and/or the length of the interlamellar traverses. The decrease in crystallinity with decreasing $\bar{M}_n$ at low $\bar{M}_n$ would occur if C is greater than U.

Epoxidation of dilute-solution-grown lamellas of *trans*-1,4-polybutadiene and *trans*-1,4-polyisopropene in suspension at low temperature has been used to assess the average number of monomer units per fold indirectly from the fraction epoxidized and the lamellar thickness[5,14-17] or directly by ^{13}C NMR analysis of the resulting block copolymer.[33] For the epoxidation method to give an accurate determination, all of the double bonds in the folds and between lamellas must react and penetration of the crystalline parts must not occur. If the fraction epoxidized exceeds the noncrystalline fraction as determined by density, then crystal penetration has probably taken place. It is also assumed that penetration and reaction of the crystalline portion will be slower than reaction of the folds, chain ends, and interlamellar links and therefore should be detectable in a fraction of double bonds reacted vs. time plot. From the results obtained in this investigation using hedrites in the α-form, complete penetration of the noncrystalline parts apparently does not occur at $[MCPBA]_{t=0}$

of 0.6 and below. At higher $[MCPBA]_{t=0}$ and polymer concentration penetration of the crystal core of at least some parts of the lamellas can take place during epoxidation. It is concluded that essentially all of the noncrystalline material present can be reacted. Therefore the intramolecular defects are not appreciable and the density values can be used as a first approximation to calculate the average number of monomer units in a noncrystalline chain sequence, U, made up of folds and interlamellar links as done above.

Acknowledgment. This research was supported by grants from the National Science Foundation, Polymers Program (Grant No. DMR-8007226), and the Professional Staff Conference—Board of Higher Education of the City University of New York (Grant No. 13148).

Registry No. Polyisoprene (homopolymer), 9003-31-0.

References and Notes

(1) Schlesinger, W.; Leeper, H. M. *J. Polym. Sci.* **1953**, *11*, 203.
(2) Keller, A.; Martuscelli, E. *Makromol. Chem.* **1972**, *151*, 189.
(3) Flanagan, R. D.; Rijke, A. M. *J. Polym. Sci., Part A-2* **1972**, *10*, 1207.
(4) Anandakumaran, K.; Kuo, C. C.; Mukherji, S.; Woodward, A. E. *J. Polym. Sci., Polym. Phys. Ed.* **1982**, *20*, 1669.
(5) Anandakumaran, K.; Herman, W.; Woodward, A. E. *Macromolecules* **1983**, *16*, 563.
(6) Bunn, C. W. *Proc. R. Soc. London, Ser. A* **1942**, *180*, 40.
(7) Fisher, D. *Proc. Phys. Soc. London* **1953**, *66*, 7.
(8) Takahashi, Y.; Sato, T.; Tadokoro, H.; Tanaka, Y. *J. Polym. Sci., Polym. Phys. Ed.* **1973**, *11*, 233.
(9) Leeper, H. M.; Schlesinger, W. *J. Polym. Sci.* **1953**, *11*, 307.
(10) Geil, P. H. "Polymer Single Crystals"; Wiley: New York, 1963.
(11) Wunderlich, B. "Macromolecular Physics"; Academic Press: New York, 1973; Vol. 1.
(12) Andrews, E. H.; Owen, P. J.; Singh, A. *Proc. R. Soc. London, Ser. A* **1971**, *324*, 79.
(13) Davies, C. K. L.; Long, O. E. *J. Mater. Sci.* **1977**, *12*, 2165.
(14) Stellman, J. M.; Woodward, A. E. *J. Polym. Sci., Part B* **1969**, *7*, 755.
(15) Wichacheewa, P.; Woodward, A. E. *J. Polym. Sci., Polym. Phys. Ed.* **1978**, *16*, 1849.
(16) Tseng, S.; Herman, W.; Woodward, A. E.; Newman, B. A. *Macromolecules* **1982**, *15*, 338.
(17) Tseng, S.; Woodward, A. E. *Macromolecules* **1982**, *15*, 343.
(18) Cooper, W.; Vaughan, G. *Polymer* **1963**, *4*, 329.
(19) Fischer, E.; Henderson, J. F. *J. Polym. Sci., Part A-2* **1967**, *5*, 377.
(20) Woodward, A. E. *Polymer* **1964**, *5*, 293.
(21) Khoury, F.; Barnes, J. D. *J. Res. Natl. Bur. Stand., Sect. A* **1972**, *76*, 225.
(22) Khoury, F.; Barnes, J. D. *J. Res. Natl. Bur. Stand., Sect. A* **1974**, *78*, 95.
(23) Barnes, J. D.; Khoury, F. *J. Res. Natl. Bur. Stand. Sect. A* **1974**, *78*, 363.
(24) Maxfield, J.; Mandelkern, L. *Macromolecules* **1977**, *10*, 550.
(25) Allen, R. C.; Mandelkern, L. *J. Polym. Sci., Polym. Phys. Ed.* **1982**, *20*, 1465.
(26) Davies, C. K. L.; Long, O. E. *J. Mater. Sci.* **1979**, *14*, 2529.
(27) Hamada, F.; Wunderlich, B.; Sumida, T.; Hayashi, S.; Makajima, A. *J. Phys. Chem.* **1968**, *72*, 178.
(28) Banks, W.; Gordon, M.; Roe, R.-J.; Sharples, A. *Polymer* **1963**, *4*, 61.
(29) Maclaine, J. Q. G.; Booth, C. *Polymer* **1975**, *16*, 680.
(30) Se, K.; Adachi, K.; Kotaka, T. *Polym. J.* **1981**, *13*, 1009.
(31) Marco, C.; Fatou, J. G.; Bello, A. *Polymer* **1977**, *18*, 1100.
(32) Marco, C.; Fatou, J. G.; Bello, A.; Blanco, A. *Polymer* **1979**, *20*, 1250.
(33) Schilling, F. C.; Bovey, F. A.; Tseng, S.; Woodward, A. E. *Macromolecules* **1983**, *16*, 808.

Forces between Two Adsorbed Poly(ethylene oxide) Layers in a Good Aqueous Solvent in the Range 0–150 nm

Jacob Klein*† and Paul F. Luckham

Physics and Chemistry of Solids, Cavendish Laboratory, Cambridge, CB3 0HE U.K.
Received August 29, 1983

ABSTRACT: We have measured the forces $F(D)$ between two smooth curved mica surfaces a distance D apart immersed in 0.1 M KNO_3, both in the absence and in the presence of adsorbed layers of monodispersed poly(ethylene oxide), of two molar masses M (40 000 and 160 000). Interactions between the bare surfaces are characteristic of electrostatic double-layer overlap, and strongly repulsive for $D \lesssim 8$ nm. Following adsorption of the polymer, the main features of the interactions are as follows: (i) On a first approach of the surfaces following adsorption and on subsequent compression/decompression cycles that are sufficiently slow to allow relaxation of the polymer on the surfaces ($\gtrsim$1 h), a *quasi-equilibrium* $F(D)$ profile is indicated. The onset of repulsive interactions occurs at $D \simeq 6 \pm 1\ R_g$ (the respective radii of gyration for the two molar masses), and $F(D)$ is increasingly repulsive at lower D values. (ii) More rapid ($\sim$5 min) compression/decompression cycles reveal time-dependent effects. The general observation in these cases is that $F(D)$ is lower for any given D than the corresponding quasi-equilibrium value. (iii) The adsorbance of polymer is 4 ± 1.5 mg m^{-2}, and adsorption is irreversible over the times of our experiments. (iv) There is no evidence for attraction or adhesion between the surfaces once the equilibrium adsorption has been attained. Our results contrast with an earlier report for a similar system but utilizing a commercial-grade polymer (Israelachvili et al. *J. Colloid Interface Sci.*, 78, 432 (1980)), in particular as regards our observations of an equilibrium force–distance profile.

Introduction

The use of adsorbed macromolecules to stabilize colloidal dispersions (e.g., inks and paints) has a long history, and such steric stabilization has been intensively studied over the past few decades.[1] Most of these studies have involved the investigation of conditions under which polymer-coated colloidal dispersions retain (or lose) their stability, while only very few, relatively recently, have attempted to measure directly steric interaction forces between adsorbed macromolecular layers.[2-4]

Surface-balance[5] and compression-cell[6] techniques have been used to measure the pressure between colloidal particles in two- and three-dimensional arrays. More recently, van Vliet and Lyklema[2] measured the disjoining pressure between layers of polymers adsorbed at the two liquid–air interfaces of a film of polymer solution as a function of film thickness; Cain et al.[3] measured the force as a function of distance between layers of polymers adsorbed onto silicon rubber spheres, using the rubber de-

† Also Polymer Department, Weizmann Institute, Rehovot, Israel.

0024-9297/84/2217-1041$01.50/0